Systems/Circuits

Differential Contributions of Ventral Striatum Subregions to the Motivational and Hedonic Components of the Affective Processing of Reward

Eva R. Pool,[1,2*] David Munoz Tord,[1,2,3*] Sylvain Delplanque,[1,2] Yoann Stussi,[1,2,4] Donato Cereghetti,[5] Patrik Vuilleumier,[1,6] and David Sander[1,2]

[1]Swiss Center for Affective Sciences, University of Geneva, 1202 Geneva, Switzerland , [2]E3 Lab, Department of Psychology, Faculté de Psychologie et des Sciences de l'Education, University of Geneva, 1211 Geneva, Switzerland, [3]Department of Psychology, Formation Universitaire à Distance Suisse, 3900 Brigue, Switzerland, [4]Department of Psychology, Harvard University, Cambridge, Massachusetts 02138, [5]Firmenich, Geneva 1242, Switzerland, and [6]Department of Fundamental Neuroscience, University of Geneva, Switzerland

The ventral striatum is implicated in the affective processing of reward, which can be divided into a motivational and a hedonic component. Here, we examined whether these two components rely on distinct neural substrates within the ventral striatum in humans (11 females and 13 males). We used a high-resolution fMRI protocol targeting the ventral striatum combined with a pavlovian-instrumental task and a hedonic reactivity task. Both tasks involved an olfactory reward, thereby allowing us to measure pavlovian-triggered motivation and sensory pleasure for the same reward within the same participants. Our findings show that different subregions of the ventral striatum are dissociable in their contributions to the motivational versus the hedonic component of the affective processing of reward. Parsing the neural mechanisms of the interplay between pavlovian incentive and hedonic processes may have important implications for understanding compulsive reward-seeking behaviors such as addiction, binge eating, or gambling.

Key words: **affective processing; high-resolution fMRI; olfactory reward; pavlovian instrumental transfer; sensory pleasure; ventral striatum**

Significance Statement

Reward deeply shapes learning, memory, and decision-making. What makes reward such an efficient signal is its affective dimension, the processing of which critically relies on the ventral striatum. Decades of research in affective neuroscience have shown that reward processing can be parsed into motivational and hedonic components. Our findings show that different ventral striatal subregions distinctly contribute to these components in humans; the pavlovian motivation relied on the core-like division, whereas the sensory pleasure relied on the shell-like division. This evidence for a functional heterogeneity of the ventral striatum in reward affective processing has important implications for the understanding of this key brain structure and the development of targeted interventions for affective disorders such as addiction.

Introduction

It is widely held that the ventral striatum (VS) is implicated in reward processing. Findings have highlighted its role in the computation of reward prediction errors (O'Doherty et al., 2003) and in the anticipation of reward delivery (Knutson et al., 2001). The VS has also been consistently implicated in the affective processing of rewarding stimuli (Cardinal et al., 2002; Delgado, 2007; Wang et al., 2016). Affective processes involved in reward processing are often categorized into motivational and hedonic mechanisms. The motivational mechanisms determine how much effort an individual mobilizes to obtain a reward, whereas the hedonic mechanisms determine how much pleasure an individual experiences during reward consumption (Berridge and Kringelbach, 2015).

Received June 3, 2021; revised Dec. 7, 2021; accepted Jan. 1, 2022.

Author contributions: E.R.P., S.D., P.V., and D.S. designed research; E.R.P. and Y.S. performed research; S.D. and D.C. contributed unpublished reagents/analytic tools; E.R.P., D.M.T., and S.D. analyzed data; E.R.P., D.M.T., and Y.S. wrote the paper.

This work was supported by a research grant (EmOdor, project UN9046) from Firmenich to D.S. and P.V. This study was conducted on the imaging platform at the Brain and Behavior Lab with support from the technical staff. We thank Dr. Leonardo Ceravolo for the discussion on the analysis, Dr. Vanessa Sennwald for insightful comments on the manuscript. The authors would also like to acknowledge the precious contribution and support at the early stages of this project of our colleague and friend Dr. Charlotte Prévost who passed away in March of 2016.

*E.R.P. and D.M.T. contributed equally to this work.

The authors declare no competing financial interests.

Correspondence should be addressed to Eva R. Pool at eva.pool@unige.ch.

https://doi.org/10.1523/JNEUROSCI.1124-21.2022

The VS itself is not a unitary and homogeneous structure. Studies conducted on rodents typically distinguish between the anatomically distinct core (i.e., dorsolateral) and shell (i.e., ventromedial) nuclei. The human VS is also known to be heterogeneous, but its subdivision into core and shell is not as well defined. However, recent work based on tractographic connectivity suggests that a similar parcellation might also exist in humans, distinguishing between core-like and shell-like subregions within the human VS (Xia et al., 2017; Cartmell et al., 2019). This VS segmentation might be relevant to the affective processing of reward in humans as studies conducted in rodents have demonstrated that the core and shell divisions are differentially involved in the functional processing of motivational and hedonic mechanisms, respectively (Corbit and Balleine, 2011; Berridge and Kringelbach, 2015).

Animals studies have outlined the critical role of the VS in reward motivational processes, particularly in pavlovian-triggered motivation (Corbit and Balleine, 2011; Wassum et al., 2013). This type of motivation is usually tested using a paradigm called pavlovian-instrumental transfer (PIT).

In this paradigm, a pavlovian stimulus associated with the reward typically triggers a motivational response enhancing the execution of an instrumental action associated with that reward. This phenomenon (in its general form) notably relies on the activity of the VS core division (Corbit and Balleine, 2011). Strikingly, a critical role of the VS has also been demonstrated in hedonic processes (Peciña and Berridge, 2005; Berridge and Kringelbach, 2015). These hedonic reactions can be amplified by an opioid or endocannabinoid stimulation of so-called hedonic hotspots (Berridge and Kringelbach, 2015; Castro and Berridge, 2017), which have been found in the shell division of the VS (Peciña and Berridge, 2005).

A growing number of studies have extended animal findings regarding the role of the VS in pavlovian motivation to humans by adapting the PIT paradigm to an MRI scanner (Talmi et al., 2008; Chen et al., 2020; Schad et al., 2020). In contrast, the findings suggesting the human VS is involved in sensory pleasure remain less consistent. Similar to animals, hedonic expressions in humans appear to be modulated by opioidergic activity (Korb et al., 2020). However, whereas some studies find that the magnitude of the experienced sensory pleasure correlates with the activity of the VS (Kühn and Gallinat, 2012; Weber et al., 2018), sensory pleasure has been most consistently reported to correlate with the activity of the medial orbitofrontal cortex (mOFC; Kringelbach, 2005; Zou et al., 2016). Meta-analytical investigations have notably found the VS to be more implicated in the anticipation of the reward and the mOFC to be more implicated in the reward consumption (Diekhof et al., 2012). This discrepancy might arise from the fact that the hedonic hotspots in the shell division are relatively small (Berridge and Kringelbach, 2015), implying that the standard spatial resolution of functional magnetic resonance imaging (fMRI) protocols might not be able to reliably detect the hedonic signal from this region in humans.

In the present study, we deployed a high-resolution fMRI protocol to test the hypothesis that the motivational and hedonic components of the affective processing of reward rely on distinct subregions of the VS in humans. We combined a human-adapted PIT task (Talmi et al., 2008; Pool et al., 2015) with a hedonic reactivity task using the same olfactory reward for both tasks, thereby enabling us to measure directly and separately the pavlovian-triggered motivation and the sensory pleasure experience for the same reward within the same participants.

Materials and Methods

Participants

We recruited 26 healthy participants at the University of Geneva. Participants were screened to exclude (1) those with any previous history of neurologic/psychiatric disorders, (2) those with any kind of olfactory disorder, and (3) those who were on a diet or seeking to lose weight. Moreover, participants were screened to include only those who perceived the chocolate odor used as a reward as pleasant. Data from two participants were excluded because of technical problems with their fMRI scans (one participant could not enter the scanner because of a piercing, and the images from the other participant could not be used because the table moved during the scanning session). We therefore used the data from the remaining 24 participants (11 females, age 26.56 $\pm$ 4.72 years). Participants were asked to fast for 6 h before each experimental session. They gave their written informed consent and were paid 60 Swiss francs for their participation. The study protocol was approved by the Regional Research Ethics Committee in Geneva (protocol number 15-015). The sample size was determined based on previous studies using similar high-resolution sequences on subcortical brain regions and similar tasks (Prévost et al., 2012, 2013; Pauli et al., 2015, 2019).

Odor stimuli and presentation

The 12 olfactory stimuli (Aladinate, Cassis, Ghee, Indol, Leather, Paracresol, Pin, Pipol, Popcorn, Methyl salicylate, Yogurt, and Chocolate) were provided by Firmenich. All odorants were diluted (20% v/v) in dipropylene glycol (DIPG), the control condition (odorless air) consisted of pure DIPG. The olfactory stimuli were selected based on pleasantness evaluations done in previous pilot studies on a visual analog scale going from 0 (extremely unpleasant) to 100 (extremely pleasant). The 11 neutral olfactory stimuli were selected based on their evaluations being more or less neutral (varying from mean = 39 and SD = 21 to mean = 66 and SD = 16), and the chocolate olfactory stimulus was selected to be used as the olfactory reward because it was consistently evaluated as being very pleasant (mean = 82 and SD = 3).

The odors were delivered directly to the participants' nostrils through a computer-controlled olfactometer with an air flow fixed at 1.5 L/min via a nasal cannula. There was a constant odorless air stream delivered throughout the experimental session, and the odorant molecules were delivered in this air stream without any change in the overall flow rate. The olfactory stimuli were thereby delivered rapidly and without thermal or tactile confounds, thus avoiding any change in the somatosensory stimulation (Ischer et al., 2014).

Mobilized effort

The mobilized effort was measured through an fMRI-compatible isometric handgrip (catalog #TDS121C) connected to the MP150 system (Biopac Systems) with a 500 Hz sampling rate. The dynamic value of the signal used to provide participants with an online visual feedback (Psychtoolbox 3.0 for the visual interface implemented in MATLAB version 8.0) that reflected the force exerted on the handgrip. This visual feedback was illustrated through the mercury of a thermometer-like image displayed on the left side of the screen (30° visual angle) that moved up and down according to the effort mobilized (Fig. 1). The mercury of the thermometer-like display reached the top if the handgrip was squeezed with at least 50 or 70% (criterion varied every 1 s) of the participants' maximal force. Note that we also recorded electromyographical activity from the zygomaticus and the corrugator muscles of the face of our participants. However, we could not systematically retrieve the signal of these recordings in the noise generated by the fMRI environment and therefore did not include these results here. This data are nonetheless available with the rest of the data presented here.

Experimental design

The experiment consisted of two separate testing days (Fig. 1). The first day was conducted outside the scanner; participants underwent the instrumental learning task, the pavlovian learning task, and an odor selection task. The second day was conducted inside the scanner, where the participants underwent the PIT test and the hedonic reactivity task. The PIT task included three phases; an instrumental learning task, a

pavlovian learning task, and a transfer test. During instrumental learning, an instrumental action (i.e., squeezing a handgrip) was first associated with an olfactory reward (unconditioned stimulus). Subsequently, during pavlovian learning, fractal images were either associated with the delivery of the olfactory reward [positively conditioned stimulus (CS+)] or with odorless air [negatively conditioned stimulus (CS−)]. The learning of the contingencies between the CSs and the olfactory outcomes was assessed through reaction times in a key-press task and liking ratings of the CSs (Gottfried et al., 2003; Talmi et al., 2008; Pool et al., 2015). In the final transfer test, the effort mobilized on the handgrip was measured during the presentation of the pavlovian stimuli (Fig. 1), the test was administered under extinction, so the olfactory reward was not delivered over this time. In this task, participants smelled the rewarding odor, a neutral odor, and odorless air multiple times. They were asked to report how pleasant the experience of smelling the odor was at that particular time. The 2 days design allowed us to optimize the time participants spent inside the scanner, limiting fatigue effects. Moreover, it allowed us to reduce the amount of odor exposure, limiting saturation and contamination effects. The transfer test (assessing the motivational component of the reward) and the hedonic reactivity task (assessing the hedonic component of the reward) were administered the same day.

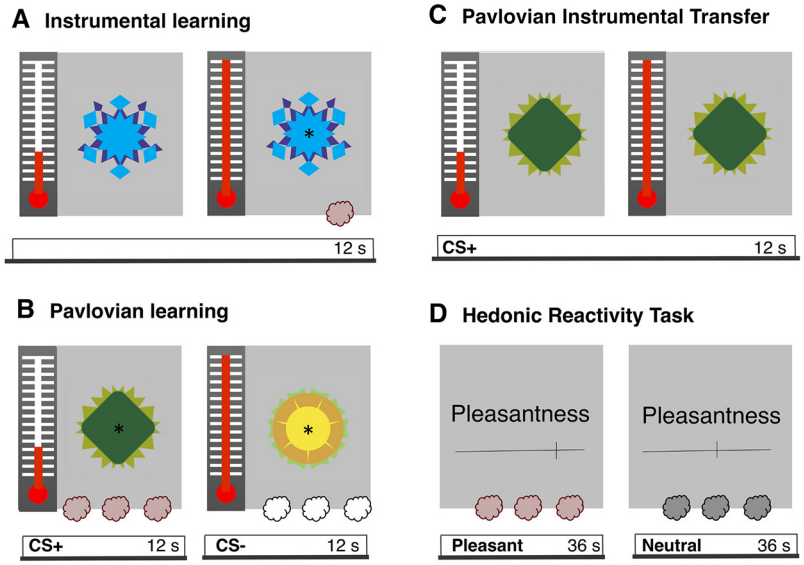

Figure 1. Illustration of the methodological procedure. ***A***, ***B***, During day 1, participants underwent instrumental and pavlovian learning outside the scanner. During instrumental learning (***A***), participants learned to associate an instrumental action with an outcome. More precisely, they learned to squeeze a handgrip to trigger the release of the olfactory reward. During pavlovian learning (***B***), participants learned to associate two visual stimuli with the presence or the absence of an outcome. More precisely, they were exposed to repeated pairings of the CS+ with the olfactory reward, whereas the CS− was paired with odorless air. ***C***, ***D***, During day 2 participants underwent a PIT test and a hedonic reactivity task inside the scanner. The PIT test (***C***) was administered under extinction. The CS+ and the CS− were displayed in random order (here, a CS+ trial is illustrated), and participants could squeeze the handgrip if they wished to do so. The PIT task was adapted from Talmi et al. (2008). During the hedonic reactivity task (***D***), participants were presented with the olfactory reward, a neutral odor, and odorless air. They were asked to evaluate on a visual analog scale their perception of the pleasantness (from 0, extremely unpleasant, to 100, extremely pleasant) and the intensity (from 0, not perceived, to 100, extremely strong) of the odor.

Instrumental conditioning. In this task, participants learned to associate an instrumental action with an outcome. More precisely, participants learned to squeeze a handgrip to trigger the release of the olfactory reward (same procedure as Pool et al., 2015). There were 24 trials (12 s) followed by an intertrial interval (ITI) of 4–12 s. During the trial, a fractal image (8° visual angle) and a thermometer were displayed in the center and on the left side of the screen, respectively (Fig. 1*A*). Note that the fractal image used during the instrumental conditioning was different from the three fractal images used during pavlovian conditioning and was never used as a CS in the pavlovian conditioning procedure. The fractal image was the same across all the instrumental trials so that participants could focus on the action–outcome contingencies only. The fluid movement of the thermometer-like mercury display provided online visual feedback of the effort participants exerted on the handgrip. Participants were asked to squeeze the handgrip, thereby bringing the mercury of the thermometer up to the maximum and then down again, without paying attention to their squeezing speed. They were told that during the presentation of the thermometer display, there were three special 1 s windows and that if they happened to squeeze the handgrip during one of these time windows, they would trigger the release of the olfactory reward. They were also told that they were free to choose when to squeeze the handgrip and were encouraged to use their intuition. In reality, only two 1 s windows were randomly selected in each trial to be rewarded with the olfactory reward. If participants squeezed the handgrip with at least 50 or 70% (criterion varied every 1 s) of their maximal force during these time windows, a sniffing signal (a black asterisk; 2° visual angle) was displayed at the center of the fractal image, and the olfactory reward was delivered. During the ITI, a fixation cross (2° visual angle) was displayed at the center of the screen, and participants were asked to relax their hand to recalibrate their baseline force.

Pavlovian conditioning. Participants learned to associate a visual stimulus with the presence or the absence of an outcome. More precisely, they learned to associate a fractal image with the delivery of the olfactory reward and another fractal image with the delivery of odorless air. Three initially neutral fractal images were attributed the pavlovian roles of baseline, CS+ and CS−. The pavlovian role of the fractal images was counterbalanced across participants. Each image was displayed at the center of the screen (visual angle of 8°). There were 36 trials (12 s) during which the CS+ or the CS− was displayed on the screen, followed by an ITI (12 s) during which the baseline image was displayed (procedure from Pool et al., 2015). During each trial, a target appeared every 4 s (on average) at the center of the CS image, three times per trial (Fig. 1*B*). Participants had to press the A key as fast as possible after they perceived the target, which was presented for a maximum of 1 s. Each time the CS+ image was displayed and the participant pressed the key, an olfactory reward was released; when the CS− image was displayed, odorless air was released. Participants were informed that the kind of odor released depended only on the CS image and not on the key-press task. In fact, the odor was released 1 s after the target onset when participants did not press the key during this interval. They were told about this aspect, and it was moreover emphasized that the key-press task was a measure of their sustained attention and independent of the image-odor contingencies (Talmi et al., 2008). Offline, however, reaction times were used as an indirect measure of pavlovian learning. During the ITI, the baseline image was displayed without any target, and no odor was released. After pavlovian conditioning, participants evaluated the pleasantness of the images used as CS+, CS−, and baseline on a visual analog scale (from extremely unpleasant to extremely pleasant) presented at the center of the computer screen (visual angle of 23°). The order of the images was randomized across participants. These ratings were used as a measure of pavlovian learning at the self-report level.

Odor selection task. Participants evaluated the pleasantness (from extremely unpleasant to extremely pleasant) and the intensity (from not perceived to extremely strong) of the 11 neutral odors, the olfactory reward, and the odorless air on visual analog scales displayed on a computer screen. Among the neutral odors, the odor rated as the most neutral (the closest to 50) and with the most similar intensity to the olfactory reward was selected to be used on the second day in the scanner for each participant.

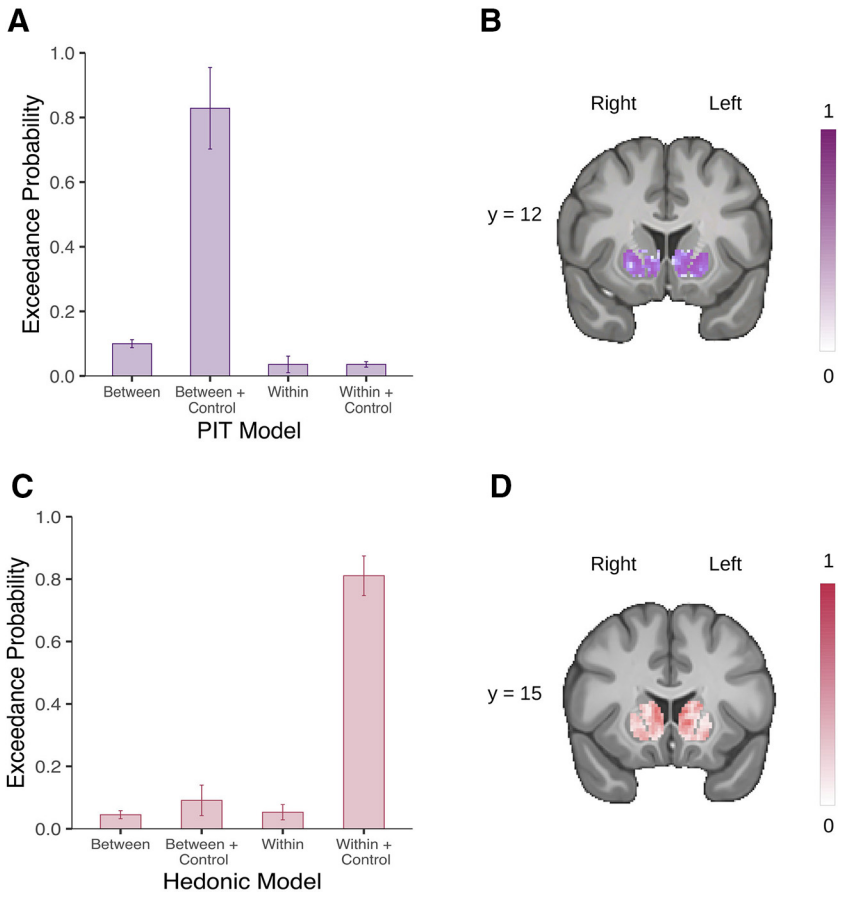

Figure 2. Voxel-wise Bayesian model selection in the striatum. ***A***, Mean exceedance probability across voxels within the striatum for the PIT models. ***B***, Likeliest frequency map of the winning PIT model (Between + Control). ***C***, Mean exceedance probability across voxels within the striatum for the hedonic models. ***D***, Likeliest frequency map of the winning hedonic model (Within + Control). Scale bars show the proportion of subjects in which the winning model is the optimal model. Error bars indicate ±1 SD.

PIT. The transfer test was administered on the second day while participants were lying in the scanner. Participants were instructed to perform the same instrumental task as the day before by squeezing the handgrip and keeping their gaze on the fractal image presented at the center of the screen. First, they completed three trials identical to those in instrumental conditioning (two special 1 s windows were rewarded), followed by six trials administered under partial extinction (one special 1 s window was rewarded). Immediately afterward, they performed the transfer test trials administered under extinction (no time window was rewarded). In the transfer test, the pavlovian fractal images (CS+, CS−, or baseline) replaced the instrumental fractal image. The presentation order of the transfer test trials was randomized across the three stimuli (CS+, CS−, and baseline). There were five cycles of testing. In each cycle, each cue was presented three times consecutively so that each of the pavlovian stimuli was presented 15 times for a total of 45 transfer trials. The difference in instrumental responding during the CS+ and the CS− was used as an index of the PIT effect, and the trial-by-trial trajectory of this difference across the extinction trials reflected the within-participants variability.

Hedonic reactivity task. The hedonic reactivity task was administered after the PIT while participants were still lying in the scanner. Participants evaluated the pleasantness (from extremely unpleasant to extremely pleasant) and the intensity (from not perceived to extremely strong) of the three odor stimuli (rewarding, neutral, and odorless). Each odor release was preceded by a 3 s countdown, and when the odor was released, the sniffing cue was presented at the center of the screen for 2.5 s. Afterward, the ratings were done on visual analog scales displayed on a computer screen, and participants had to answer through a button box placed in their hand. The answer to the question was self-paced, and the time participants took to answer was removed from the duration of the ITI (12 s). There were 54 trials (18 per odor) consisting of six randomized cycles of presentation for each condition where the odor was administered three consecutive times per cycle.

Statistical analysis

Behavioral data. Statistical analyses of the behavioral data were performed with R (version 4.0; https://www.r-project.org/). For the ANOVAs, we used the afex (https://www.rdocumentation.org/packages/afex/versions/1.0-1) and BayesFactor (https://cran.r-project.org/web/packages/BayesFactor/BayesFactor.pdf) packages. Adjustments of degrees of freedom using Greenhouse–Geisser correction were applied when the sphericity assumption was not met. We computed the Bayes factor (BF_{10}) quantifying the likelihood of the data under the alternative hypothesis relative to the likelihood of the data under the null hypothesis using Bayesian ANOVAs (Rouder et al., 2012). The Bayes factors reported for the main effects compared the model with the main effect in question versus the null model, whereas the Bayes factors reported for the interaction effects compared the model including the interaction term to the model including all the other effects but the interaction term. Partial η squared (η_p^2) or Cohen's d_z and their 90 or 95% confidence interval (CI) are reported as estimates of effect sizes for the ANOVAs and the t tests, respectively.

fMRI data

Acquisition parameters. Because animal studies suggest that the hedonic hotspots in the shell division of the VS are relatively small (Berridge and Kringelbach, 2015), we deployed a high-resolution protocol for the recording of functional imaging. In recent years, high-resolution fMRI sequences have been developed for the investigation of subcortical regions in reward processing (Prévost et al., 2012, 2013; Colas et al., 2017; Pauli et al., 2019, 2015), facilitating the investigation of the role of different nuclei in various subcortical structures and the translation of classical animal findings to humans (Prévost et al., 2012; Pauli et al., 2015).

Acquisition was performed at the Brain and Behavior Laboratory (University of Geneva) using a 3-Tesla MRI system (Magnetom Tim Trio, Siemens) with a 32-channel receive array head coil for all the MR scanning sessions. The acquisition of the neuroimaging data was performed according to a high-resolution fMRI sequence from Prévost et al. (2012). We recorded 26 echoplanar imaging (EPI) slices per scan with an isotropic voxel size of 1.8 mm. Note that this volume is 4.6 times smaller than a fairly standard fMRI resolution with 3 mm isotropic voxels. Our scanner parameters were set at TE = 41 ms, TR = 2400 ms, FOV = 180 × 180 × 39.6 mm, matrix size = 100 × 100 voxels, flip angle = 75°, no gap between slices. Because of our a priori regions of interest (ROIs), the acquired partial oblique axial T2*-weighted ($T2^*_w$) EPI mainly covered the striatum and the OFC. The field of view was determined before the tasks and adjusted for each participant. We also acquired whole brain T1-weighted ($T1_w$) images (isotropic voxel size = 1.0 mm), a whole brain reference functional image for the coregistration of the images, and dual-echo gradient B_0 field maps to allow geometric correction of the EPI data.

Preprocessing. We combined the Oxford Center Functional MRI of the Brain (FMRIB) Software Library (FSL; version 4.1; Jenkinson et al., 2012) with the Advanced Normalization Tools (ANTS, version 2.1; Avants et al., 2011) to tailor the preprocessing of high-resolution fMRI

data for subcortical structures. FSL was used for brain extraction and realignment of functional images. The functional images were automatically denoised using an independent components analysis and hierarchical fusion of classifiers (ICA-FIX). To achieve higher accuracy, the ICA-FIX classifier was trained on the present dataset. Field maps were applied to correct geometric distortion (FMRIB Utility for Geometrically Unwarping EPIs). ANTS was used to diffeomorphically coregister the preprocessed functional and structural images to the California Institute of Technology (CIT168) brain template in the Montreal Neurological Institute (MNI) space, using nearest-neighbor interpolation and leaving the functional images in their native 1.8 mm isometric resolution (Pauli et al., 2019). Finally, we applied a spatial smoothing of 4 mm full-width at half-maximum (FWHM).

Model selection and analysis. The Statistical Parametric Mapping software (version 12; Penny et al., 2011) was used to perform a random-effects univariate analysis on the voxels of the image times series following a two-stage approach to partition model residuals to take into account within- and between-participant variance (Holmes and Friston, 1988; Mumford and Poldrack, 2007). For the first level, we specified a general linear model (GLM) for each participant. We used a high-pass filter cutoff of 1/128 Hz to eliminate possible low-frequency confounds (Talmi et al., 2008). Each regressor of interest was derived from the onsets and duration of the stimuli and convoluted using a canonical hemodynamic response function into the GLM to obtain weighted parameter estimates.

We used a Bayesian model selection (BMS) to select the best GLM given our data for our group-level analysis. This procedure allowed us to compute the probability of the data given the model (model evidence) for a set of candidate models. For each task, we created several GLMs with an increasing level of complexity, and we performed model comparisons between the different GLMs using the Model Assessment, Comparison, and Selection toolbox (Soch and Allefeld, 2018). First, we estimated the cross-validated log model evidence for subject-level maps for each GLM, which we used to perform a random-effects BMS following the procedure suggested in Stephan et al. (2009), extended to voxel-wise estimation (Soch et al., 2016). Finally, we selected the final model based on the averaged group-level exceedance probability maps across voxels within the striatum (Fig. 2). Group-level statistic *t* maps were then created for each task by combining subject-level contrasts.

The multiple comparisons correction was done using the Analysis of Functional magnetic resonance NeuroImages software (version 20.2; Cox, 1996). First, we used the 3dFWHMx function to estimate the intrinsic spatial smoothness of each dimension separately. Then, we used the new 3dClustSim function (Cox et al., 2017) to create–via Monte Carlo simulation to form those estimates—a cluster extent threshold corrected for multiple comparisons at $p < 0.05$ for a height threshold of $p < 0.005$ within the ROI. We report the extent threshold (k^{thr}), the weighted parameter estimate (β), and the number of consecutive significant voxels at $p < 0.005$ within the cluster (k).

On account of our hypothesis, we used anatomic gray matter masks to define our a priori ROIs for cluster correction. We chose this method to remain faithful to the structural brain architecture. For the analysis testing of our hypothesis of interest, we used cytoarchitectural maps (Henssen et al., 2016) to identify the mOFC and the Harvard-Oxford atlas to identify the VS. For the control analyses testing the quality of our signal, we used cytoarchitectural maps (Henssen et al., 2016) to identify the cerebellum, as well as the thalamus, and the parcellation from Zhou et al. (2019) for the olfactory cortex. We display nonmasked statistical *t* maps of our group results overlaid on a high-resolution template (CIT168) in MNI space.

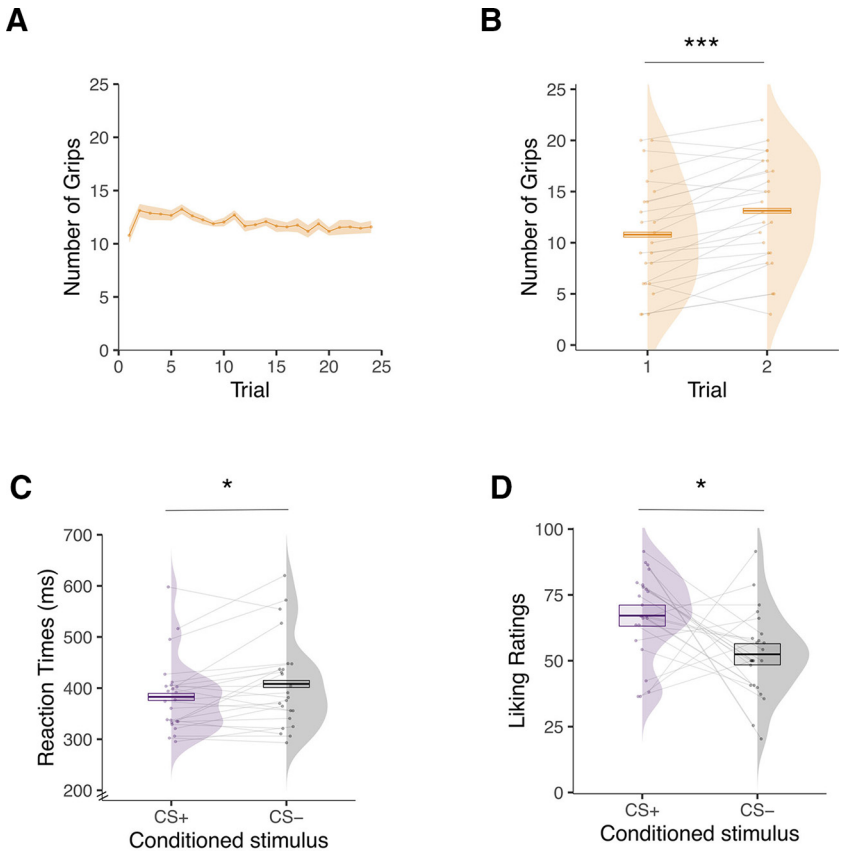

Figure 3. Behavioral results for day 1 outside the scanner. ***A***, Mean number of squeezes on the handgrip during the instrumental learning task displayed as a function of trials over time. ***B***, Mean number of squeezes on the handgrip during the first and second trial of the instrumental learning task. ***C***, Mean reaction times to detect an asterisk while the conditioned stimulus associated with the olfactory reward (CS+) or odorless air (CS−) was presented during the pavlovian learning task. ***D***, Mean liking ratings (from 0, extremely unpleasant, to 100, extremely pleasant) of the fractal images used as CS+ and CS− during the pavlovian learning task. Error bars indicate ±1 SEM, adjusted for within-participants designs. Asterisks indicate statistically significant differences between conditions (*$p < 0.05$, ***$p < 0.001$).

Finally, to further investigate the different involvement of the nuclei within the VS, we used the core-like and shell-like segmentations of the human VS created by Cartmell et al. (2019) based on a diffusion-tractography analysis of 245 participants. We used those probabilistic maps to test whether the average activation within the core-like and shell-like divisions would map onto the motivational and hedonic components of the affective processing of the reward, respectively.

Univariate test of pavlovian-triggered motivation. We build four possible GLMs and used the BMS to select the one that was the most sensitive to variations in the striatum. The first GLM (*Between*) consisted of the following six regressors: (1) the onsets of the reminder phase, (2) the onsets of the partial extinction phase, (3) the onsets of the PIT CS+, (4) the onsets of the PIT CS−, (5) the onsets of the PIT baseline, and (6) a parametric regressor of noninterest encompassing the phasic handgrip activity for each volume to account for residual movement. The second GLM (*Between+control*) was similar to the first one, but we added a control regressor of noninterest to account for the repetition of the presentation of the same CS. The third GLM (*Within*) included the same regressors as the first GLM with an additional parametric modulator encompassing the force exerted on the handgrip during the presentation of the pavlovian fractal images, whereas the fourth GLM (*Within+control*) additionally included the control regressor of noninterest to account for the repetition presentation of the same CS.

Results of the BMS showed that the second GLM had the best fit within the striatum (Fig. 2*A*). The main group-level contrast was derived from the

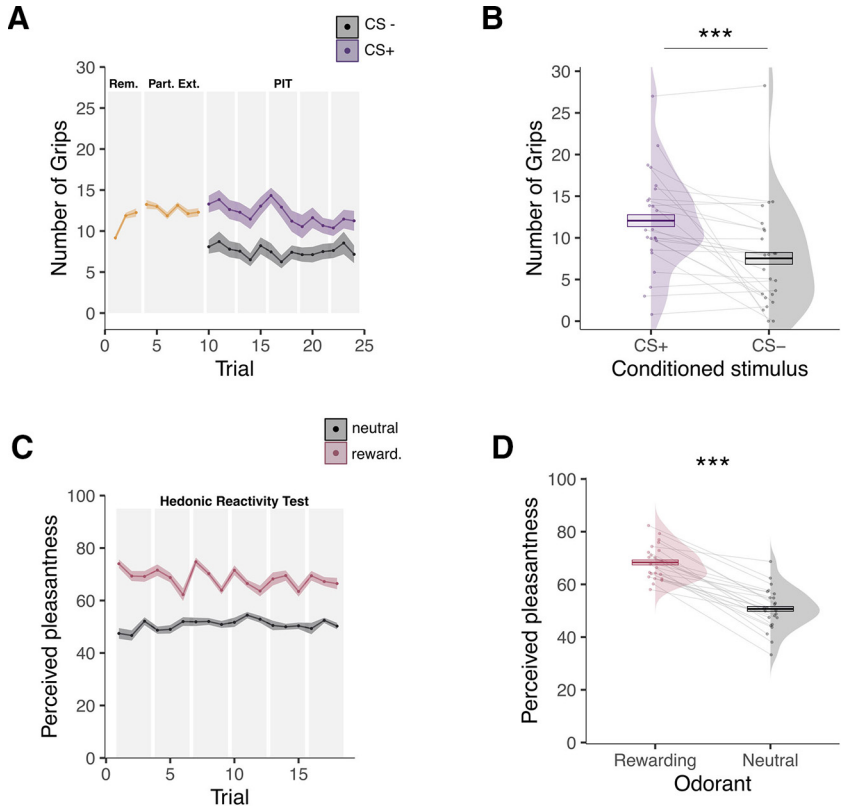

Figure 4. Behavioral results for day 2 inside the scanner. ***A***, Mean number of squeezes as a function of trials over time during the PIT test. The first 10 trials consisted of a reminder (Rem.) of the instrumental contingencies and a partial extinction (Part. Ext.); the rest of the trials consisted of the actual PIT test for which the number of squeezes is depicted separately for the conditioned stimulus previously associated with the olfactory reward (CS+) and the conditioned stimulus previously paired with odorless air (CS−). ***B***, Overall mean number of squeezes while the CS+ or the CS− was presented during the PIT test. ***C***, Mean perceived pleasantness ratings as a function of trials over time depicted separately for the rewarding and the neutral odors during the hedonic reactivity task. ***D***, Overall mean perceived pleasantness of the rewarding and the neutral odors. Pleasantness was evaluated on a scale from 0 (extremely unpleasant) to 100 (extremely pleasant). Error bars indicate ±1 SEM, adjusted for within-participants designs. Asterisks indicate statistically significant differences between conditions (***$p < 0.001$).

linear difference between the CS+ and the CS− conditions correlated with the behavioral PIT effect. The behavioral PIT effect was computed by taking each participant's average number of squeezes exerted during the CS+, to which we subtracted the average in the CS− condition, which we rank transformed because of non-normality.

Finally, a control GLM was also computed with the onsets of every single squeeze during the whole task independently of the experimental condition. This aimed to validate our task and to control the quality of the BOLD signal by verifying whether the main effect of squeezing frequency activated motor regions included in our field of view.

Univariate test of the pleasure experience. We built four possible GLMs and used BMS to select the one that was the most sensitive to variations in the striatum. The first GLM (*Between*) consisted of the following six regressors: (1) the onsets of the trial, (2) the onsets of the reception of the pleasant odor, (3) the onsets of the reception of the neutral odor, (4) the onsets of the reception of the odorless air, (5) the onsets of the question about odor pleasantness, and (6) the onsets of the question about odor intensity. The second GLM (*Between+control*) was similar to the first one, but we added a control regressor of noninterest to account for the repetition of the presentation of the same odor. The third GLM (*Within*) consisted of the following seven regressors: (1) the onsets of the trial, (2) the onsets of the reception of an odor modulated by (3) the trial-by-trial ratings of the perceived pleasantness, (4) the trial-by-trial ratings of the perceived intensity, (5) the onsets of the reception of the odorless air, (6) the onsets of the question about odor pleasantness, and (7) the onsets of question about odor intensity. The two modulators locked on the onset of the odor reception were competing for variance so that they would each represent their individual explained variance (Mumford et al., 2015). The fourth GLM (*Within+control*) was identical to the third one, but we added two additional regressors of noninterest accounting for the repetition of the presentation of the same odor and whether the odor presented at a given trial was more or less pleasant than that of the preceding trial.

Results of the BMS showed that the fourth GLM had the best fit within the striatum (Fig. 2*C*). The main group-level contrast was derived from the parametric modulation of pleasantness on the odor reception.

Finally, a control GLM was also computed with the onset of the reception of the odors and the onset of the odorless air reception, as well as the perceived intensity of the odors as a second-level modulator. This aimed at validating our task and quality control of the BOLD signal by verifying whether the main effect of odor activated the olfactory regions in our field of view.

Code and data accessibility

Raw, de-identified MRI data are available from the Open Neuro platform (openneuro.org/datasets/ds003487). Computer code used for preprocessing and analyzing the data are available from a publicly hosted software repository (github.com/evapool/VS_AffectiveResponse).

Results

Behavioral results

Instrumental Conditioning

To test for instrumental learning, we applied a repeated-measures ANOVA to the number of squeezes surpassing 50% of each participant's maximal force (Talmi et al., 2008; Pool et al., 2015) over 24 trials. The analysis did not reveal a statistically significant effect of trial ($F_{(5.08,116.84)} = 1.54$, $p = 0.181$, $\eta_p^2 = 0.06$, 90% CI = [0.00, 0.11], $BF_{10} = 0.133$; Fig. 3*A*). A *post hoc* test revealed very rapid learning, showing that participants significantly increased their responding from the first (mean = 10.79, SD = 5.34) to the second trial (mean = 13.12, SD = 5.22; $F_{(1,23)} = 24.77$, $p < 0.001$, $\eta_p^2 = 0.52$, 90% CI = [0.27, 0.68], $BF_{10} = 312.54$; Fig. 3*B*).

Pavlovian Conditioning

To test for pavlovian learning, we analyzed the reaction times (in ms) of the key-press task and the liking ratings of the CS images. For the key-press task, we analyzed the reaction times on the first target during the task-on period (Pool et al., 2015). All responses that were >3 SD from each participant's mean or absent (2.54% of the trials) were removed. Participants showed evidence of learning in the reaction times. They were faster to detect the target when the CS+ image (mean = 382.84, SD = 87.52) was presented compared with when the CS− image (mean = 408.16, SD = 72.19) was presented ($F_{(1,23)} = 6.67$, $p = 0.017$, $\eta_p^2 = 0.22$, 90% CI = [0.03, 0.45], $BF_{10} = 3.08$; Fig. 3*C*). Participants also showed evidence of learning in the liking ratings. They rated the CS+ image (mean = 67.13, SD = 16.11) as more pleasant than the CS− image (mean = 52.44, SD = 16.08; $F_{(1,23)} = 6.70$, $p = 0.016$, $\eta_p^2 = 0.23$, 90% CI = [0.03, 0.45], $BF_{10} = 18.01$; Fig. 3*D*).

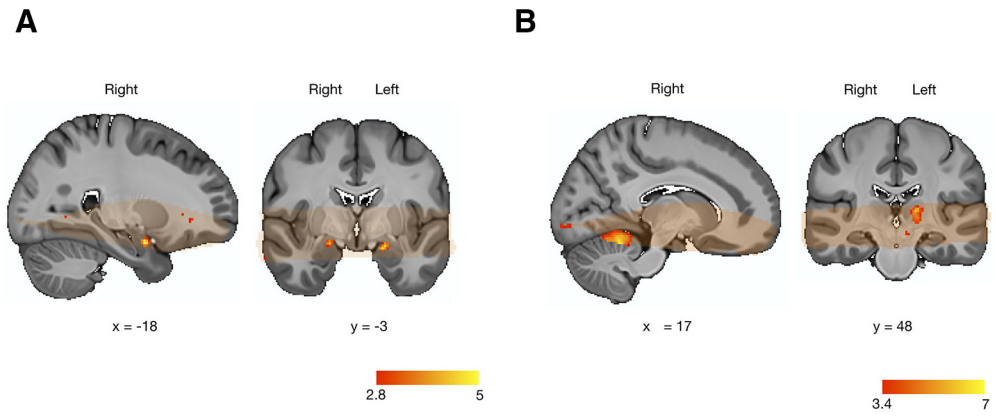

Figure 5. Olfactory and motor signals in the hedonic reactivity task and the PIT task. ***A***, An olfactory signal was found in the bilateral piriform cortex during the hedonic reactivity task. ***B***, For display purposes, statistical *t* maps are shown with a threshold at $p < 0.005$, uncorrected. A motor signal was found in the right cerebellum and the left thalamus during the PIT task. For display purposes, statistical *t* maps are shown with a threshold at $p < 0.001$, uncorrected. Orange overlays indicate brain areas from which fMRI data were acquired in all participants and were thus included in the statistical analysis. Scale bar indicates *t* statistic.

PIT Task

We analyzed the number of squeezes surpassing 50% of each participant's maximal force (Talmi et al., 2008; Pool et al., 2015) during the transfer test in a 2 (image, CS+ or CS−) × 15 (extinction trials) repeated-measures ANOVA. Participants mobilized more effort when the CS+ image (mean = 12.06, SD = 5.92) was displayed compared with when the CS− image (mean = 7.54, SD = 6.30) was displayed ($F_{(1,23)} = 13.58$, $p < 0.001$, $\eta_p^2 = 0.37$, 90% CI = [0.12, 0.57], $BF_{10} = 29.79$; Fig. 4*A*,*B*). There was no statistically significant effect of trial ($F_{(5.07,116.52)} = 1.39$, $p = 0.23$, $\eta_p^2 = 0.06$, 90% CI = [0.00, 0.10], $BF_{10} = 0.074$) or interaction between trial and CS image ($F_{(5.31,122.13)} = 0.99$, $p = 0.43$, $\eta_p^2 = 0.04$, 90% CI = [0.00, 0.07], $BF_{10} = 0.004$; Fig. 4*A*). To further investigate the effects of extinction, we ran an analysis by splitting the trials into an early (first seven trials) and a late (last seven trials) phase. We ran a 2 (image, CS+ or CS−) × 2 (extinction trials, early or late) repeated-measures ANOVA. The analysis showed an interaction between image and extinction trials ($F_{(1,23)} = 7.43$, $p = 0.012$, $\eta_p^2 = 0.24$, 90% CI = [0.04, 0.46], $BF_{10} = 0.432$). *Post hoc* tests showed that the number of squeezes in response to the CS+ was higher during early versus late extinction ($F_{(1,23)} = 5.80$, $p = 0.024$, $\eta_p^2 = 0.20$, 90% CI = [0.02, 0.43], $BF_{10} = 2.31$). By contrast, the number of squeezes in response to the CS− did not statistically differ between early and late extinction ($F_{(1,23)} = 0.26$, $p = 0.616$, $\eta_p^2 = 0.01$, 90% CI = [0.00, 0.16], $BF_{10} = 0.317$).

Hedonic Reactivity Task

We analyzed the pleasantness ratings during the hedonic reactivity task with a 2 (odor, rewarding or neutral) × 18 (trial) repeated-measures ANOVA. As expected, participants rated the olfactory reward (mean = 68.33, SD = 6.37) as more pleasant than the neutral odor (mean = 50.69, SD = 7.87); $F_{(1,23)} = 136.66$, $p < 0.001$, $\eta_p^2 = 0.98$, 90% CI = [0.97, 0.99], $BF_{10} = 4.1 \times 10^9$; Fig. 4*B*,*C*). The analysis additionally showed a main effect of trial ($F_{(8.42,205.52)} = 4.29$, $p = 0.028$, $\eta_p^2 = 0.09$, 90% CI = [0.01, 0.12], $BF_{10} = 3.06$; Fig. 4*C*) and an interaction between odor and trial ($F_{(8.94,205.52)} = 4.29$, $p < 0.001$, $\eta_p^2 = 0.16$, 90% CI = [0.06, 0.21], $BF_{10} = 5790.33$; Fig. 4*C*). A follow-up analysis showed that the perceived pleasantness of an odor at trial t was influenced by the value of the preceding odor at trial t-1. The olfactory reward was rated as more pleasant when it was preceded by the neutral odor compared with when it was preceded by another olfactory reward ($F_{(1.35,31.08} = 97.43$, $p < 0.001$, $\eta_p^2 = 0.81$, 90% CI = [0.70, 0.87], $BF_{10} = 3.01 \times 10^{15}$). A second follow-up analysis, testing a linear contrast of trials for the reward condition, highlighted a reward saturation effect, indicating that the reward was rated as less pleasant over trial repetitions ($F_{(1,23} = 6.256$, $p = 0.019$, $\eta_p^2 = 0.21$, 90% CI = [0.02, 0.44], $BF_{10} = 2.89$). Despite this reward saturation effect, the olfactory reward was still perceived as largely more pleasant than the neutral odor in the last trial of the hedonic reactivity task ($F_{(1,23} = 43.10$, $p < 0.001$, $\eta_p^2 = 0.65$, 90% CI = [0.44, 0.77], $BF_{10} = 1.77 \times 10^5$).

Because the neutral and rewarding odors were selected during day 1 (outside the scanner) to have similar intensities, we also analyzed the intensity ratings during the hedonic reactivity task as a control. Participants rated the olfactory reward (mean = 52.11, SD = 12.40) as more intense than the neutral odor (mean = 39.40, SD = 16.45; ($F_{(1,23)} = 15.87$, $p < 0.001$, $\eta_p^2 = 0.41$, 90% CI = [0.15, 0.60], $BF_{10} = 73.96$). There was also a main effect of trial ($F_{(7.90,181.80)} = 9.25$, $p < 0.001$, $\eta_p^2 = 0.29$, 90% CI = [0.18, 0.35], $BF_{10} = 3.06$), but no statistically significant interaction between odor and trial emerged ($F_{(8.46,194.61)} = 0.94$, $p = 0.49$, $\eta_p^2 = 0.04$, 90% CI = [0.00, 0.05], $BF_{10} = 0.002$). A follow-up analysis showed that the odor at trial t was perceived as more intense when it was preceded by a different odor at trial t-1 compared with when it was preceded by the same odor at trial t-1 ($F_{(1,23} = 57.74$, $p < 0.001$, $\eta_p^2 = 0.72$, 90% CI = [0.53, 0.81], $BF_{10} = 4060.65$).

fMRI results

Tasks Validation

Before focusing on our hypotheses in ROIs, we validated our paradigms and the quality of our signal through two control analyses. We report the results from our analyses within predefined ROIs in the olfactory cortex, the cerebellum, and the thalamus using a height threshold of $p < 0.005$, with an extent threshold significant at $p < 0.05$, corrected for multiple comparisons. For the hedonic reactivity task, the odor presence (odor > odorless air) activated the piriform bilaterally ($k^{thr} = 18$; right, MNI *x*, *y*, *z* = 25, −3, −20; $k = 89$, $\beta = 0.54$, 95% CI = [0.37, 0.70], SE = 0.079; left, MNI *x*, *y*, *z* = −23, −7, −10; $k = 47$, $\beta = 0.52$, 95% CI = [0.32, 0.71], SE = 0.096; Fig. 5*A*). For the PIT task, the overall frequency of the squeezes executed with the right hand activated the motor regions in our field of view, consisting of the right cerebellar hemisphere ($k^{thr} = 44$; MNI *x*, *y*, *z* = 18,

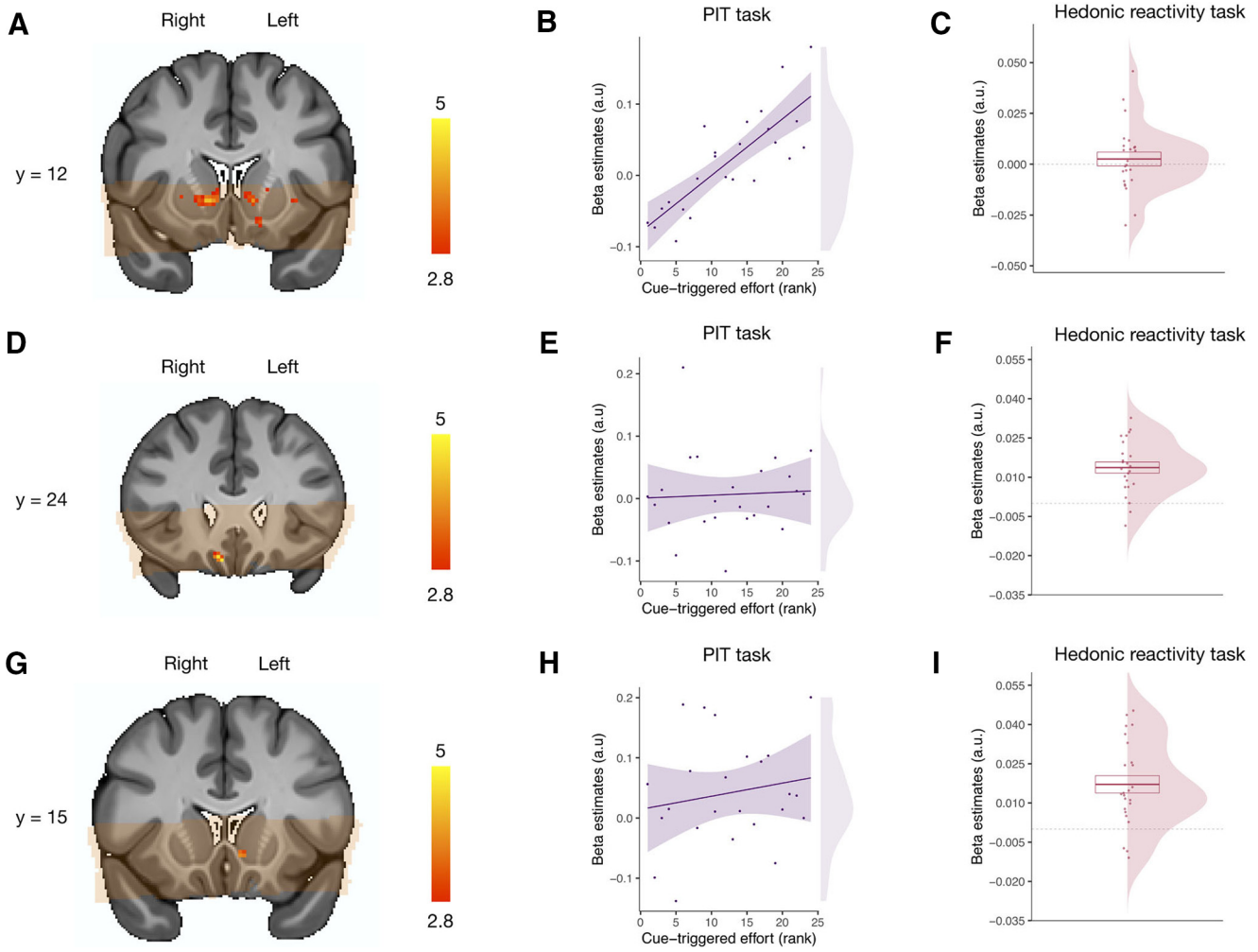

Figure 6. Neural correlates of pavlovian-triggered motivation and of sensory pleasure. ***A***, BOLD signal positively correlating with the magnitude of the PIT effect across participants in the VS. ***B***, Scatter plot showing the pavlovian β estimates (CS+ > CS−) extracted from the voxels within the VS correlating with the PIT effect against the strength of the behavioral PIT for each participant. ***C***, Overall mean across participants of the hedonic β estimates (pleasure modulator) extracted from the voxels within the VS correlating with the PIT effect. ***D***, BOLD signal positively correlating with the magnitude of the hedonic pleasure experienced within participants in the mOFC. ***E***, Scatter plot showing the pavlovian β estimates (CS+ > CS−) extracted from the voxels within the mOFC correlating with the hedonic experience against the strength of the behavioral PIT for each participant. ***F***, Overall mean across participants of the hedonic β estimates (pleasure modulator) extracted from the voxels within the mOFC correlating with the hedonic experience. ***G***, BOLD signal positively correlating with the magnitude of the hedonic pleasure experienced within participants within the VS. ***H***, Scatter plot showing the pavlovian β estimates (CS+ > CS−) extracted from the voxels within the VS correlating with the hedonic experience against the strength of the PIT effect for each participant. ***I***, Overall mean across participants of the hedonic β estimates (liking) extracted from the voxels within the VS correlating with the hedonic experience. Orange overlay indicates from which brain areas the fMRI data were acquired in all participants and were thus included in the statistical analysis. For display purposes, statistical *t* maps are shown with a threshold of $p < 0.005$, uncorrected. Scale bar shows *t*-statistic. Error bars indicate ±1 SEM adjusted for within-participants designs.

−48, −18; $k = 1128$, $\beta = 1.04$, 95% CI = [0.70, 1.38], SE = 0.164; Fig. 5*B*), and the left thalamus, ($k^{thr} = 37$; MNI *x*, *y*, *z* = −16, −20, 7; $k = 168$, $\beta = 0.45$, 95% CI = [0.32, 0.59], SE = 0.065; Fig. 5*B*).

PIT Task

We report the results from our analyses within the predefined ROI in VS and mOFC using a height threshold of $p < 0.005$, with an extent threshold significant at $p < 0.05$ corrected for multiple comparisons. Following the between-participants analysis typically used in PIT tasks (Talmi et al., 2008; Prévost et al., 2012), we extracted the CS+ versus CS− contrast for each participant at the first level and correlated it with the average PIT effect (increased effort during the CS+ compared with the CS−) of each participant at the second level.

For this contrast, we did not find any statistically significant activation in the mOFC, but as shown in Figure 6, *A* and *B*, we found a bilateral activation of the dorsolateral subregion of the VS ($k^{thr} = 16$; left, MNI *x*, *y*, *z* = −18, 23, −4; $k = 69$, $\beta = 0.11$, 95% CI = [0.080, 0.15], SE = 0.017; right, MNI *x*, *y*, *z* = 13, 13, −2; $k = 159$, $\beta = 0.12$, 95% CI = [0.085, 0.16], SE = 0.017).

To test whether those voxels that were activated for the PIT or were also implicated in sensory pleasure, we extracted the β estimates from these voxels during the hedonic reactivity task for our most sensitive pleasure contrast. These β estimates were not statistically different from 0 ($t_{(23)} = 0.76$, $p = 0.45$, $d_z = 0.16$, 95% CI = [−0.25, 0.57], $BF_{10} = 0.002$; Fig. 6*C*).

Hedonic Reactivity Task

We report the results from our analyses within the predefined ROI in VS and mOFC using a height threshold of $p < 0.005$, with an extent threshold significant at $p < 0.05$, corrected for multiple comparisons. Following the within-participants analysis typically used in hedonic reactivity tasks (Kringelbach et al., 2003), we extracted the contrast correlating with the trial-by-trial

experienced pleasantness reported by the participants. We found a statistically significant activation in the right mOFC (k^{thr} = 10; MNI *x*, *y*, *z* = 9, 25, −18; *k* = 22, β = 0.013, 95% CI = [0.0093, 0.018], SE = 0.0021; Fig. 6*D*,*F*). Moreover, we also found a significant activation in the left ventromedial subregion of the VS (k^{thr} = 15; MNI *x*, *y*, *z* = −5, 13, −5; *k* = 19, β = 0.017, 95% CI = [0.010, 0.024], SE = 0.0033; Fig. 6 *D*,*F*).

To test whether those voxels that were activated for sensory pleasure were also implicated in the PIT, we extracted the β estimates (CS+ > CS−) from these clusters during the PIT task and correlated them with each participant's PIT effect (increased effort during the CS+ compared with the CS−). This analysis did not reveal any statistically significant effect for the voxels in the mOFC ($F_{(1,22)}$ = 0.06, p = 0.81, η_p^2 = 0.01, 90% CI = [0.00, 0.11], BF_{10} = 0.59; Fig. 6*E*) or for the voxels in the VS ($F_{(1,22)}$ = 0.69, p = 0.42, η_p^2 = 0.03, 90% CI = [0.00, 0.22], BF_{10} = 0.67; Fig. 6*H*).

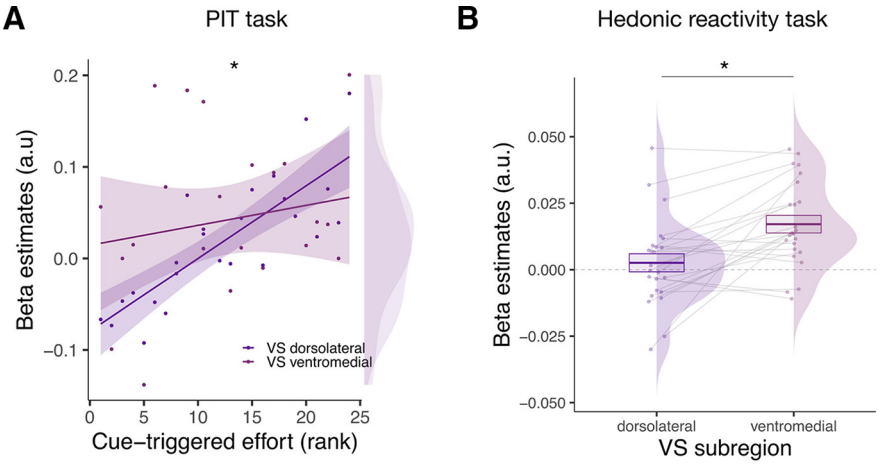

Figure 7. Direct comparison of the ventral striatum subregions during the hedonic reactivity task and the PIT task. ***A***, Scatter plot showing the pavlovian β estimates (CS+ > CS−) extracted from the voxels within the VS subregions (dorsolateral and ventromedial) correlating with the PIT effect against the strength of the behavioral PIT for each participant. ***B***, Overall mean across participants of the hedonic β estimates (pleasure modulator) extracted from the different VS subregions (dorsolateral and ventromedial). Asterisks indicate statistically significant differences between conditions (*$p < 0.05$). Error bars indicate ± 1 SEM adjusted for within-participants designs.

Direct comparison of Ventral Striatum Subregions

To directly compare the activity of two subregions within the VS during the hedonic and the PIT task, we entered the β values reflecting the activation of these regions in two separate statistical models for each experimental task. First, we compared the activity of the ventromedial and the dorsolateral striatum during the PIT task. We ran a GLM on the betas extracted during the PIT task (CS+ > CS−) in which we entered ROI (left ventromedial VS or bilateral dorsolateral VS) as a dichotomous factor and the magnitude of the PIT effect across participants as a continuous factor. This analysis revealed a statistically significant interaction between the subregions of the VS and the magnitude of the PIT effect ($F_{(1,22)}$ = 6.58, p = 0.018, η_p^2 = 0.23, 90% CI = [0.03, 0.46], BF_{10} = 4.28), suggesting that the dorsolateral subregion of the VS was more involved in the PIT than the left ventromedial subregion of the VS (Fig. 7*A*). Second, we compared the activity of the ventromedial and the dorsolateral striatum during the hedonic task. We ran a GLM on the betas extracted during the hedonic reactivity task in which we entered ROI (left ventromedial VS or bilateral dorsolateral VS) as a dichotomous factor. This analysis revealed a main effect of ROI ($F_{(1,23)}$ = 4.79, p = 0.039, η_p^2 = 0.17, 90% CI = [0.01, 0.40], BF_{10} = 2.80), now suggesting that the left ventromedial subregion of the VS was more involved in the sensory pleasure than the dorsolateral subregion of the VS (Fig. 7*B*).

Pavlovian-Triggered Motivation and Sensory Pleasure Within the Core-Like and Shell-Like Divisions

To further test the differential contribution of the core and shell nuclei of the VS, we used these two ROIs as defined by Cartmell et al., (2019). We expected our general PIT effect to correlate with the activity of the core-like division and the sensory pleasure experience to correlate with the shell-like division.

First, we tested the implication of the core-like division in the PIT effect by extracting the β estimates (CS+ > CS−) from within this ROI during the PIT task and correlating them with the PIT effect of each participant (increased effort during the CS+ compared with the CS−). This analysis showed a statistically significant effect for the voxels in the core ($F_{(1,22)}$ = 10.63, p = 0.004, η_p^2 = 0.33, 90% CI = [0.08, 0.51], BF_{10} = 7.75; Fig. 8*B*). To test whether the core-like division was also implicated in sensory pleasure, we extracted the β estimates from the core-like ROI during the hedonic reactivity task for our most sensitive pleasure contrast (see above, Materials and Methods). These β estimates were not statistically different from 0 ($t_{(23)}$ = 0.76, p = 0.35, d_z = 0.19, 95% CI = [−0.21, 0.60], BF_{10} = 0.32).

Second, we tested whether the shell-like division was involved in sensory pleasure by extracting the β estimates from this ROI during the hedonic reactivity task. These β estimates were statistically different from 0 ($t_{(23)}$ = 2.28, p = 0.032, d_z = 0.47, 95% CI = [0.03, 0.88], BF_{10} = 1.85; Fig. 8*C*). To test whether the shell was also implicated in the PIT effect, we extracted the β estimates (CS+ > CS−) from the shell-like division during the PIT task and correlated them with the PIT effect of each participant (increased effort during the CS+ compared with the CS−). This analysis did not reveal any statistically significant effect for the voxels in the shell-like division ($F_{(1,22)}$ = 2.04, p = 0.17, η_p^2 = 0.08, 90% CI = [0.00, 0.29], BF_{10} = 0.92).

Discussion

This study investigated whether, different subregions of the human VS are differentially involved in the motivational and hedonic components of the affective processing of reward. With this aim, we combined a high-resolution fMRI protocol with a PIT task and a hedonic reactivity task using an olfactory reward to try to maintain the paradigms as similar as possible to those used in animal research. This allowed us to measure pavlovian-triggered motivation and the sensory pleasure experience for the same reward within the same participants. Our findings showed evidence of dissociable contributions of different subregions of the VS to motivational and hedonic processes of reward. More specifically, when comparing between core-like and shell-like segmentation of the VS, our findings suggest that the pavlovian-triggered motivation relies on the core-like division, whereas the sensory pleasure experience relies on the shell-like division of the VS, and on the mOFC.

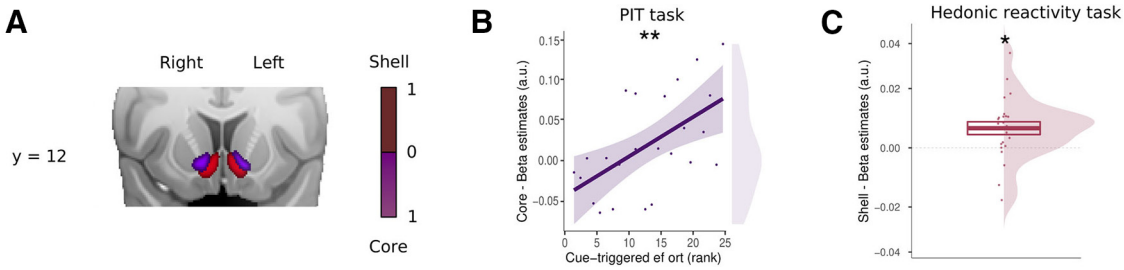

Figure 8. Pavlovian-triggered motivation and sensory pleasure within the core-like and shell-like divisions of the ventral striatum. ***A***, Probabilistic atlas from Cartmell et al. (2019) depicting the core-like (in purple) and shell-like (in red) divisions of the human ventral striatum. Scale bar indicates the probability of the presence of a given division. ***B***, Scatter plot showing the pavlovian β estimates (CS+ > CS−) extracted from the core-like division of the ventral striatum against the strength of the PIT effect for each participant. ***C***, Overall mean across participants of the hedonic β estimates (liking) extracted from the shell-like division of the ventral striatum. SEM adjusted for within-participants designs. Asterisks indicate statistically significant differences (*$p < 0.05$, **$p < 0.01$). Error bars indicate ± 1 SEM adjusted for within-participants designs.

Our study showing the involvement of the VS in pavlovian-triggered motivation accords with findings from previous studies conducted in rodents (Wyvell and Berridge, 2001; Corbit and Balleine, 2011; Wassum et al., 2013) and humans (Talmi et al., 2008; Chen et al., 2020; Van Timmeren et al., 2020). The VS has long been demonstrated to be implicated in PIT effects in rodents (Wyvell and Berridge, 2001; Corbit and Balleine, 2011; Wassum et al., 2013), with evidence of a dissociation between the shell and the core divisions underlying two distinct forms of PIT, the outcome-specific and the general effects, respectively (Corbit and Balleine, 2011). During the outcome-specific PIT effects, a pavlovian stimulus exerts a selective influence only invigorating a specific instrumental action associated with a specific reward. During the general PIT effects, a pavlovian stimulus triggers the invigoration of any instrumental responding, regardless of the specific reward associated with the instrumental action (Corbit and Balleine, 2015). Although fMRI studies conducted in humans have found a correlation between the VS and global PIT effects (Chen et al., 2020; Van Timmeren et al., 2020), they have typically reported an activation of the dorsal striatum for outcome-specific effects (Bray et al., 2008; Prévost et al., 2012). Our version of the PIT task did not allow us to distinguish between these two forms of pavlovian influence on the instrumental action. Nonetheless, the generic form of this task we used is likely to reflect a general PIT effect (Cartoni et al., 2016), which is congruent with the activation we observed in core-like division of the VS. Importantly, the activation of the VS we found during our task also replicates findings from a previous study in humans using the same version of the task with a monetary reward (Talmi et al., 2008). It is, however, important to note that there is a difference between our results and the results of the aforementioned study. Whereas Talmi et al. (2008) found the VS to be correlated with the PIT effect within participants, we found the VS to be correlated with the magnitude of the PIT effect between participants. This difference could be driven by the behavior of our participants. Unlike Talmi et al. (2008), we did not observe a strong effect of extinction during the PIT task. Therefore, our data showed less within-participant variability in terms of the PIT effect. By contrast, we observed a large variability in the magnitude of the PIT effect between participants, which provided the variance for the brain-behavior correlation analysis.

More generally, our findings highlighting the role of the more dorsolateral regions of the VS in reward motivation effects are congruent with prior work in the human fMRI literature showing that the dorsolateral striatum mediates the impact of the affective properties of a reward on the instrumental action (Delgado et al., 2004; Delgado, 2007). They moreover stress that the involvement of the VS extends to the caudate in conditions with incentive actions and stimulus-driven motivational states (Knutson et al., 2001; Pauli et al., 2016). Importantly, our findings further contribute to identifying the preferential involvement of the dorsolateral subregion of the VS in underlying the motivational component, as opposed to the hedonic component, of the affective processing of reward.

An important feature of our study is the use of an olfactory reward. Different from other kinds of rewarding stimuli used in humans consisting in representations of rewards that will be delivered at a later stage (e.g., food pictures), olfactory rewards trigger an immediate sensory pleasure experience, which is pivotal for the empirical measure of hedonic reactions that are comparable to the animal literature (Pool et al., 2016). This allowed us to specifically compare the involvement of distinct VS subregions during the PIT task and during the sensory pleasure experience triggered by the reward consumption, thus providing evidence for a functional dissociation. This methodological feature also provides a platform for a cross-species comparison between studies conducted in rodents and in humans. Our results are in line with findings from rodent studies showing that dopamine-agonist amphetamine injections within various subregions of the nucleus accumbens amplified the PIT effect but not the hedonic response during reward consumption (Wyvell and Berridge, 2001; Peciña and Berridge, 2013). These studies have played a pivotal role in the formulation of the incentive salience hypothesis, which postulates that under some particular circumstances the motivational (i.e., wanting) and hedonic (i.e., liking) components of the affective processing of reward can be dissociated, thereby making organisms work for a reward that they will not necessarily like once obtained—a key feature of compulsive reward-seeking behaviors such as addiction (Berridge and Kringelbach, 2015). However, in contrast to studies conducted in rodents, we were not able to determine in our study whether the observed activation of the VS dorsolateral subregion is related to dopaminergic activity. Future studies might accordingly combine pharmacological manipulations with high-resolution fMRI protocols to shed more light on the neural mechanisms underlying the motivational and hedonic components of the affective processing of reward. It is important to note that there might be a caveat in the interpretation of our PIT effect in terms of pavlovian influences. Similar to Talmi et al. (2008), our pavlovian learning task involved an instrumental component (i.e., key press to discover whether the image was associated with the olfactory reward or not). However, the instrumental action had only limited predictive value in that the olfactory reward was delivered based on the CS image, and this was the case even when the

instrumental action was not performed. Therefore, pavlovian associative mechanisms were very likely to be dominant during our pavlovian learning task. Although this methodological aspect prevents us from totally excluding an influence of instrumental processes on our measure of the motivational component, we decided to use the PIT paradigm developed by Talmi et al. (2008) because we already adapted this paradigm to olfactory rewards in a prior study (Pool et al., 2015). This allowed us to have a solid behavioral basis for the investigation of the related neural mechanisms.

With respect to the hedonic component, we found the involvement of both a small subregion of the shell-like division of VS and of the mOFC in the sensory pleasure experience during the reward consumption. The involvement of the mOFC in the sensory pleasure experience has long been established in human fMRI experiments (Kringelbach, 2005; Kühn and Gallinat, 2012). By comparison, the involvement of a subregion of the VS in the sensory pleasure experience is more striking. fMRI studies conducted in humans have sometimes reported the involvement of the VS in hedonic reactions (Kringelbach, 2005; Weber et al., 2018) but less consistently than the mOFC (Zou et al., 2016). Studies conducted in rodents have highlighted the presence of small hedonic hotspots in the shell division of the VS enhancing the hedonic expression when stimulated with opioids or endocannabinoid (Peciña and Berridge, 2005). The combination of a high-resolution fMRI protocol and a hedonic reactivity task using an olfactory reward may have allowed us to detect the signal from such a small region in humans. Critically, in the hedonic reactivity task, we asked our participants to evaluate their hedonic experience during each trial. Our findings highlight the importance of this idiosyncratic measure, given that the perception of the pleasantness of the same odor varied in function of habituation (i.e., whether the odor was presented twice or more in a row) and contrast effects (i.e., whether the pleasant odor was presented after a neutral odor). Both of these sequence effects are known to have a profound influence on chemosensory perception (Zellner et al., 2003; Pellegrino et al., 2017), hence the importance of taking into account the trial-by-trial variability within each participant. Interestingly, despite the presence of strong sequence effects such as habituation and contrast effects, we found an effect of reward saturation. The perceived pleasantness was strongly influenced by the valence level of the preceding trial. It also steadily decreased over repeated presentations, but the reward remained largely more pleasant than the neutral odor even at the end of the hedonic reactivity task.

Nevertheless, there are a number of factors that limit the comparisons that can be drawn between our findings and the findings from rodent studies that deserve to be discussed. First, our hedonic reactivity task consisted in explicit self-reported hedonic evaluations rather the passive smelling with behavioral measures. It has been suggested that explicit evaluation tasks can have a different influence on hedonic activation compared with passive smelling tasks (Zou et al., 2016). Recently, it has been shown that the electromyographic signal from facial reactions during reward consumption can be successfully used as a behavioral measure of hedonic expression without using self-reports (Korb et al., 2020). Although we tried to implement such recordings in our study, the signal of these small facial movements was unfortunately not strong enough to be retrieved from the noise of the fMRI environment. Second, in our findings, we cannot determine whether the activation of the ventromedial subregion of the VS for sensory pleasure was modulated by opioids like in animals. Interestingly, a recent pharmacological study has shown that opioidergic manipulations through naltrexone led to a reduction in hedonic expression without a parallel reduction in the subjective ratings of pleasure (Korb et al., 2020). Additional studies are thus necessary to assess whether opioidergic manipulations affect the involvement of the VS in human sensory pleasure. An investigation in the human VS might be particularly challenging as the animal literature has highlighted the presence of hedonic coldspots in the nucleus accumbens shell, which are typically activated by the same ligands as the hedonic hotspots (e.g., opioids) but inhibit, rather than amplify, hedonic expressions (Peciña and Berridge, 2005; Castro and Berridge, 2014). More generally, the impact of manipulations of opioid and dopamine manipulations on human reward processing appears to be modulated by several factors, increasing the complexity of these investigations in humans (Webber et al., 2020; Meier et al., 2021). Finally, it is worth noting that we did not determine our sample size by means of a power analysis. This implies that some caution is necessary in the interpretation of the effects we report as their size could be overestimated to some degree.

Notwithstanding these caveats, our results provide evidence of dissociable contributions of the human VS subregions to the motivational and the hedonic component of the affective processing of reward. These findings are important to further our understanding of the role of the VS in affective processes related to reward in both humans and other animals. Whereas the present experiment focused on sensory pleasure, the human literature seems to suggest that more abstract pleasures, such as music, rely on partially overlapping networks (Mas-Herrero et al., 2021). Future studies will be necessary to investigate how our findings might generalize to different kinds of rewards and pleasurable experiences. A refined knowledge of these neural mechanisms might contribute to fostering novel insights into compulsive reward-seeking behaviors, where motivational processes (such as wanting) are increased despite the absence of a related increase in hedonic processes (such as liking; Berridge and Kringelbach, 2015). As pavlovian influences have been proposed to play a pivotal role in a variety of psychiatric disorders and maladaptive behaviors, including addiction, binge eating, or gambling (Huys et al., 2014; Pool et al., 2019; Wuensch et al., 2021), modeling the interplay between pavlovian incentive processes and hedonic processes could therefore have important implications for the understanding of psychological disorders.

References

Avants BB, Tustison N, Song G, Cook P, Klein A, Gee JC (2011) A reproducible evaluation of ANTs similarity metric performance in brain image registration. Neuroimage 54:2033–2044.

Berridge KC, Kringelbach ML (2015) Pleasure systems in the brain. Neuron 86:646–664.

Bray S, Rangel A, Shimojo S, Balleine B, O'Doherty JP (2008) The neural mechanisms underlying the influence of pavlovian cues on human decision making. J Neurosci 28:5861–5866.

Cardinal RN, Parkinson JA, Hall J, Everitt BJ (2002) Emotion and motivation: the role of the amygdala, ventral striatum, and prefrontal cortex. Neurosci Biobehav Rev 26:321–352.

Cartmell SC, Tian Q, Thio BJ, Leuze C, Ye L, Williams NR, Yang G, Ben-Dor G, Deisseroth K, Grill WM, McNab JA, Halpern CH (2019) Multimodal characterization of the human nucleus accumbens. Neuroimage 198:137–149.

Cartoni E, Balleine B, Baldassarre G (2016) Appetitive pavlovian-instrumental transfer: a review. Neurosci Biobehav Rev 71:829–848.

Castro DC, Berridge KC (2014) Opioid hedonic hotspot in nucleus accumbens shell: mu, delta, and kappa maps for enhancement of sweetness "liking" and "wanting. J Neurosci 34:4239–4250.

Castro DC, Berridge KC (2017) Opioid and orexin hedonic hotspots in rat orbitofrontal cortex and insula. Proc Natl Acad Sci USA 114:9125–9134.

Chen H, Nebe S, Mojtahedzadeh N, Kuitunen-Paul S, Garbusow M, Schad DJ, Rapp MA, Huys QJ, Heinz A, Smolka MN (2020) Susceptibility to interference between pavlovian and instrumental control is associated with early hazardous alcohol use. Addict Biol 26:e12983.

Colas JT, Pauli WM, Larsen T, Tyszka JM, O'Doherty JP (2017) Distinct prediction errors in mesostriatal circuits of the human brain mediate learning about the values of both states and actions: evidence from high-resolution fMRI. PLoS Comput Biol 13:e1005810.

Corbit LH, Balleine BW (2011) The general and outcome-specific forms of pavlovian-instrumental transfer are differentially mediated by the nucleus accumbens core and shell. J Neurosci 31:11786–11794.

Corbit LH, Balleine BW (2015) Learning and motivational processes contributing to pavlovian-instrumental transfer and their neural bases: dopamine and beyond. In: Behavioral neuroscience of motivation (Simpson EH, Balsam PD, eds), pp 259–289. Springer.

Cox RW (1996) AFNI: software for analysis and visualization of functional magnetic resonance neuroimages. Comput Biomed Res 29:162–173.

Cox RW, Chen G, Glen DR, Reynolds RC, Taylor PA (2017) fMRI clustering and false-positive rates. Proc Natl Acad Sci U S A 114:3370–3371.

Delgado MR (2007) Reward-related responses in the human striatum. Ann New York Acad. Sci 1104:70–88.

Delgado MR, Stenger V, Fiez J (2004) Motivation-dependent responses in the human caudate nucleus. Cereb Cortex 14:1022–1030.

Diekhof EK, Kaps L, Falkai P, Gruber O (2012) The role of the human ventral striatum and the medial orbitofrontal cortex in the representation of reward magnitude–an activation likelihood estimation meta-analysis of neuroimaging studies of passive reward expectancy and outcome processing. Neuropsychologia 50:1252–1266.

Gottfried JA, O'Doherty J, Dolan RJ (2003) Encoding predictive reward value in human amygdala and orbitofrontal cortex. Science 301:1104–1107.

Henssen A, Zilles K, Palomero-Gallagher N, Schleicher A, Mohlberg H, Gerboga F, Eickhoff SB, Bludau S, Amunts K (2016) Cytoarchitecture and probability maps of the human medial orbitofrontal cortex. Cortex 75:87–112.

Holmes A, Friston K (1998) Generalisability, random effects and population inference. Neuroimage 7:S754.

Huys QJ, Tobler PN, Hasler G, Flagel SB (2014). The role of learning-related dopamine signals in addiction vulnerability. Prog Brain Res 211:31–77.

Ischer M, Baron N, Mermoud C, Cayeux I, Porcherot C, Sander D, Delplanque S (2014) How incorporation of scents could enhance immersive virtual experiences. Front Psychol 5:1–11.

Jenkinson M, Beckmann CF, Behrens TEJ, Woolrich MW, Smith SM (2012) FSL. Neuroimage 62:782–790.

Knutson B, Adams CM, Fong GW, Hommer D (2001) Anticipation of increasing monetary reward selectively recruits nucleus accumbens. J Neurosci 21:RC159.

Korb S, Götzendorfer SJ, Massaccesi C, Sezen P, Graf I, Willeit M, Eisenegger C, Silani G (2020) Dopaminergic and opioidergic regulation during anticipation and consumption of social and nonsocial rewards. Elife 9:e55797.

Kringelbach ML (2005) The human orbitofrontal cortex: linking reward to hedonic experience. Nat Rev Neurosci 6:691–702.

Kringelbach ML, O'Doherty J, Rolls ET, Andrews C (2003) Activation of the human orbitofrontal cortex to a liquid food stimulus is correlated with its subjective pleasantness. Cereb Cortex 13:1064–1071.

Kühn S, Gallinat J (2012) The neural correlates of subjective pleasantness. Neuroimage 61:289–294.

Mas-Herrero E, Maini L, Sescousse G, Zatorre RJ (2021) Common and distinct neural correlates of music and food-induced pleasure: a coordinate-based meta-analysis of neuroimaging studies. Neurosci Biobehav Rev 123:61–71.

Meier IM, Eikemo M, Leknes S (2021) The role of mu-opioids for reward and threat processing in humans: bridging the gap from preclinical to clinical opioid drug studies. Curr Addict Rep 8:306–318.

Mumford JA, Poldrack RA (2007) Modeling group fMRI data. Soc Cogn Affect Neurosci 2:251–257.

Mumford JA, Poline J-B, Poldrack RA (2015) Orthogonalization of regressors in fMRI models. PLoS One 10:e0126255.

O'Doherty JP, Dayan P, Friston K, Critchley H, Dolan RJ (2003) Temporal difference models and reward-related learning in the human brain. Neuron 38:329–337.

Pauli WM, Larsen T, Collette S, Tyszka JM, Seymour B, O'Doherty JP (2015) Distinct contributions of ventromedial and dorsolateral subregions of the human substantia nigra to appetitive and aversive learning. J Neurosci 35:14220–14233.

Pauli WM, O'Reilly RC, Yarkoni T, Wager TD (2016) Regional specialization within the human striatum for diverse psychological functions. Proc Natl Acad Sci U S A 113:1907–1912.

Pauli WM, Gentile G, Collette S, Tyszka JM, O'Doherty JP (2019) Evidence for model-based encoding of pavlovian contingencies in the human brain. Nat. Commun 10:1099.

Peciña S, Berridge KC (2005) Hedonic hot spot in nucleus accumbens shell: where do μ-opioids cause increased hedonic impact of sweetness? J Neurosci 25:11777–11786.

Peciña S, Berridge KC (2013) Dopamine or opioid stimulation of nucleus accumbens similarly amplify cue-triggered "wanting" for reward: entire core and medial shell mapped as substrates for pit enhancement. Eur J Neurosci 37:1529–1540.

Pellegrino R, Sinding C, De Wijk R, Hummel T (2017) Habituation and adaptation to odors in humans. Physiol Behav 177:13–19.

Penny WD, Friston KJ, Ashburner JT, Kiebel SJ, Nichols TE (2011) Statistical parametric mapping: the analysis of functional brain images. Amsterdam: Elsevier.

Pool E, Brosch T, Delplanque S, Sander D (2015) Stress increases cue-triggered "wanting" for sweet reward in humans. J Exp Psychol Animal Learn Cogn 41:128–136.

Pool E, Sennwald V, Delplanque S, Brosch T, Sander D (2016) Measuring wanting and liking from animals to humans: a systematic review. Neurosci Biobehav Rev 63:124–142.

Pool ER, Pauli WM, Kress CS, O'Doherty JP (2019) Behavioural evidence for parallel outcome-sensitive and outcome-insensitive pavlovian learning systems in humans. Nat Hum Behav 3:284–296.

Prévost C, Liljeholm M, Tyszka JM, O'Doherty JP (2012) Neural correlates of specific and general pavlovian-to-instrumental transfer within human amygdalar subregions: a high-resolution fMRI study. J Neurosci 32:8383–8390.

Prévost C, McNamee D, Jessup RK, Bossaerts P, O'Doherty JP (2013) Evidence for model-based computations in the human amygdala during pavlovian conditioning. PLoS Comput Biol 9:e1002918.

Rouder JN, Morey RD, Speckman PL, Province JM (2012) Default Bayes factors for ANOVA designs. J Math Psychol 56:356–374.

Schad DJ, Rapp MA, Garbusow M, Nebe S, Sebold M, Obst E, Sommer C, Deserno L, Rabovsky M, Friedel E, Romanczuk-Seiferth N, Wittchen H-U, Zimmermann US, Walter H, Sterzer P, Smolka MN, Schlagenhauf F, Heinz A, Dayan P, Huys QJM (2020) Dissociating neural learning signals in human sign-and goal-trackers. Nat Hum Behav 4:201–214.

Soch J, Allefeld C (2018) MACS: a new SPM toolbox for model assessment, comparison and selection. J Neurosci Methods 306:19–31.

Soch J, Haynes J-D, Allefeld C (2016) How to avoid mismodelling in GLM-based fMRI data analysis: cross-validated Bayesian model selection. Neuroimage 141:469–489.

Stephan KE, Penny WD, Daunizeau J, Moran RJ, Friston KJ (2009) Bayesian model selection for group studies. Neuroimage 46:1004–1017.

Talmi D, Seymour B, Dayan P, Dolan RJ (2008) Human pavlovian-instrumental transfer. J Neurosci 28:360–368.

Van Timmeren T, Quail SL, Balleine BW, Geurts DE, Goudriaan AE, van Holst RJ (2020) Intact corticostriatal control of goal-directed action in alcohol use disorder: a pavlovian-to-instrumental transfer and outcome-devaluation study. Sci Rep 10:4949.

Wang KS, Smith DV, Delgado MR (2016) Using fMRI to study reward processing in humans: past, present, and future. J Neurophysiol 115:1664–1678.

Wassum KM, Ostlund SB, Loewinger GC, Maidment NT (2013) Phasic mesolimbic dopamine release tracks reward seeking during expression of pavlovian-to-instrumental transfer. Biol Psychiatry 73:747–755.

Webber HE, Lopez-Gamundi P, Stamatovich SN, de Wit H, Wardle MC (2020) Using pharmacological manipulations to study the role of dopamine in human reward functioning: a review of studies in healthy adults. Neurosci Biobehav Rev 120:123–158.

Weber SC, Kahnt T, Quednow BB, Tobler PN (2018) Frontostriatal pathways gate processing of behaviorally relevant reward dimensions. PLoS Biol 16:e2005722.

Wuensch L, Pool ER, Sander D (2021) Individual differences in learning positive affective value. Curr Opin Behav Sci 39:19–26.

Wyvell CL, Berridge KC (2001) Incentive sensitization by previous amphetamine exposure: increased cue-triggered "wanting" for sucrose reward. J Neurosci 21:7831–7840.

Xia X, Fan L, Cheng C, Eickhoff SB, Chen J, Li H, Jiang T (2017) Multimodal connectivity-based parcellation reveals a shell-core dichotomy of the human nucleus accumbens. Hum Brain Mapp 38:3878–3898.

Zellner DA, Rohm EA, Bassetti TL, Parker S (2003) Compared to what? Effects of categorization on hedonic contrast. Psychonomic Bulletin and Rev 10:468–473.

Zhou G, Lane G, Cooper SL, Kahnt T, Zelano C (2019) Characterizing functional pathways of the human olfactory system. Elife 8:e47177.

Zou LQ, van Hartevelt TJ, Kringelbach ML, Cheung EF, Chan RC (2016) The neural mechanism of hedonic processing and judgment of pleasant odors: an activation likelihood estimation meta-analysis. Neuropsychology 30:970–979.